Tri-Axial Accelerometer Calibration for Leveling

Tomas Thalmann, Hans Neuner[1]

Received: September 2018 / Accepted: Octomber 2018 / Published: December 2018

Abstract

IMUs (Inertial Measurement Units) are widely used in many robotics applications. Proper calibration is inevitable to ensure usable results in sensor fusion and/or other estimation methods. Numerous sensor models for IMUs can be found in literature. These are investigated from two point of views: How well can the parameters of these models be determined? And how does they influence tilt/inclination estimation with IMUs.

In the first part several sensor models differing in the number of calibration parameters are analyzed in a simulation environment. We investigate two calibration methods: a) multi-position gravity-based calibration method without the need of external equipment, and b) a calibration routine aided by an industrial robot.

In the second part the influence of these calibration parameters on tilt estimation is examined. The well-known leveling equations using accelerometer measurements of gravity for inclination angles determination are used. This method is analyzed using variance based sensitivity analysis to identify important input parameters and to optimize the model/system.

Keywords

MEMS, IMU, Accelerometer, Leveling, Calibration, Sensitivity Analysis, Tilt Estimation

[1] Dipl.-Ing. Tomas Thalmann, Univ. Prof. Dr.-Ing. Hans Neuner
FG Ingenieurgeodäsie, Dep.für Geodäsie und Geoinformation
Gußhausstraße 27-29 / E120-5
1040 Wien
Tomas.thalmann@geo.tuwien.ac.at

1. Introduction

An IMU (inertial measurement unit) consists of tri-axis accelerometer, tri-axis gyroscopes and sometimes tri-axis magnetometers. A lot of research has been done about IMUs in fields of aerospace, navigation and robotics for several years now. This is because of some unique and beneficial characteristics (compare e.g. [1] or [2]):

- high temporal resolution
- orientation estimation
- high short term accuracy
- unlimited availability due to independence of exterior environment

In the early beginnings of IMU technology it was rather expensive and unhandy in size at the same time [3]. Recent developments of MEMS (Microelectromechanical systems) dramatically reduced size, cost and power consumption [4]. This lead to an even broader scope of applications and also accelerated research [3].

Initially mainly used in navigation tasks, IMUs are now used in several applications: Augmented Reality, Indoor- and Smartphone navigation, Robotics and Mobile Mapping Systems as examples. In particular MEMS IMUs are nowadays used by the geodetic community not only for mobile mapping and navigation tasks. Especially *accelerometer leveling* from gravity sensing attracted interest. Accelerometer leveling means computation two angles roll ϕ_{nb} and pitch θ_{nb} from accelerometer readings of the gravity vector. This method has been used recently for deformation monitoring [5, 6] and frequency analysis of vibrations, e.g. [7, 8].

Another usecase of leveling with MEMS IMUs is tilt compensation of GNSS poles, see [9, 10]. Generally leveling is used in navigation and pose estimation during unaccelerated phase to stabilize attitude and to compensate gyroscope drifts. This direct measurement of the two angles ϕ_{nb} and θ_{nb} is feed into IMU strapdown computation or an integration Kalman Filter.

For all these applications of leveling (based on the acceleration measurements) mentioned here, it is important to know the stochastic model of the derived quantities and to calibrate systematic errors sufficiently. The functional model of leveling is analyzed in terms of variance and sensitivity

analysis in Section 3.

A lot of research has focused on sensor and system calibration of IMUs. There are two main questions arising when working on IMU calibration:

- Which error model to use?
- How to calibrate estimate the parameters of the chosen model?

The choice of the inertial instrument error model depends on the application/use-case and on the effect on the derived quantities [11]. This question is tackled in Section 3.

Two basic categories of calibration approaches can be distinguished: **online** and **pre-calibration**. In the first approach, parameters of the IMU error model (see Section 2) are estimated at operation time using sensor fusion (e.g. Kalman filter) with external observations, e.g. GNSS-IMU navigation. The deterministic observability of such state parameters depends on the user dynamics [11], thus is not applicable in static applications. In addition, pre-calibration should be preferred, due to the higher noise level of MEMS sensors:

- possibilities to reduce noise in static environment
- use higher precision external sensors in static environment
- danger of vibrations overlaying systematics in kinematic applications

One has to mention, that at least sensor biases should always be estimated online, since these parameters depend highly on temperature and can significantly change over time [12, 13].

Two groups of pre-calibration methods can be found in literature concerning calibration setup. The first depends on additional equipment like reference sensor (e.g. aviation grade IMU, rate tables [14, 15, 16, 17], or optical 6DOF-tracking [18]) and is generally thought to be executed in the laboratory. These mostly expensive high precision equipment might not be available [19] and is not economical for low-cost MEMS sensors [20]. We summarize these approaches as **equipment-aided** calibrations.

The other group of approaches targets suitable methods for in-field calibration. These should be feasible for end users and mostly rely on Earth's gravity. [21] first introduced the accelerometer calibration using the property: *the magnitude of the static acceleration measured must equal that of the gravity*. This group is referred to as **gravity-based** approaches. Methods based on this property have in common, that gravity $\boldsymbol{g}$ is measured in multiple quasi-static positions (attitudes). Extensive research has been carried out, differing in number of positions and the underlying estimated error models. A summary can be found in Table 1.

Table 1 Comprehensive summary of related research.

Authors	Model Parameters	# Positions
[21]	Bias and Scale	6
[22, 14, 15, 23]	Bias, Scale and Non-orthogonalities	18
[20]	Bias, Scale, Non-orthogonalities and Cross-axis sensitivities	18 and 24
[17]	Bias, Scale and Non-orthogonalities	9
[24]	Bias, Scale, Nonlinear Scale and Non-orthogonalities	24
[25, 26]	Bias, Scale and Non-orthogonalities	36-50
[19]	Bias, Scale, Non-orthogonalities and Misalignment	30

The disadvantage of gravity-based methods is the required knowledge of the local gravity at an appropriate accuracy level. Because of this and the fact that not all of the above use-cases of accelerometer leveling require exclusively calibrations procedure in-field by user, we analyzed both calibration approaches. For the equipment-aided approach we plan to incorporate an industrial robot as a reference sensor.

The remainder of this paper is organized as follows. In Section 2 several error models for accelerometer triads from literature are introduced. In Section 3 the influence of these estimated error parameters on tilt estimation using accelerometer leveling is analyzed. Based on these results gravity-based and equipment-aided calibrations approaches are compared in Section 4. Section 5 gives the conclusion and outlook.

2. Sensor Models

Several sensor models can be found in literature. They differ mainly in the modeled error parameters. The basic model for the measured accelerometer outputs (measured forces) denoted by $\boldsymbol{f}^s = [f_x^s \quad f_y^s \quad f_z^s]^T$ proposed by [21] is:

$$\boldsymbol{f}^s = \boldsymbol{S}_f \boldsymbol{f}^a + \boldsymbol{b}_f + \boldsymbol{v}_f \,, \tag{1}$$

Where $\boldsymbol{f}^a = [f_x^a \quad f_y^a \quad f_z^a]^T$ is the calibrated force vector, $\boldsymbol{b}_f = [b_x \quad b_y \quad b_z]^T$ is the offset or biases vector and

$$\boldsymbol{S}_f = \begin{bmatrix} s_x & 0 & 0 \\ 0 & s_y & 0 \\ 0 & 0 & s_z \end{bmatrix} \tag{2}$$

is the scale factor diagonal matrix and $\boldsymbol{v}_f$ is the accelerometer random noise.

The calibrated forces $\boldsymbol{f}^a$ refer to the three accelerometer sensitivity axes, thus denoted by ^{a}. Ideally these axes should be orthogonal, but due to imprecise manufacturing this is

most likely not the case. Therefore [14] extended their model to account for this non-orthogonality of the sensor sensitivity axis by introducing

$$f^b = \boldsymbol{T}_a^b f^a \,, \quad \text{with} \quad \boldsymbol{T}_a^b = \begin{bmatrix} 1 & -\alpha_{yz} & \alpha_{zy} \\ \alpha_{xz} & 1 & -\alpha_{zx} \\ -\alpha_{xy} & \alpha_{yx} & 1 \end{bmatrix} , \tag{3}$$

which transforms the sensitivity axes to the orthogonal body or IMU-frame (denoted by ^{b}) by use of 6 parameters. Here these parameters can be interpreted as "small" angles, where α_{ij} is the rotation of the *i*-th axis around the *j*-th body axis, compare Figure 1.

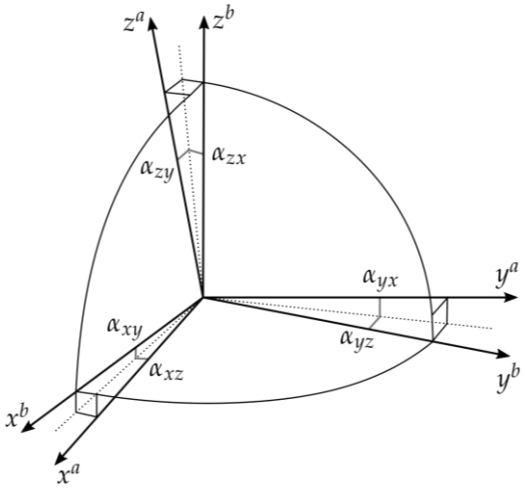

Fig. 1 The non-orthogonal sensitivity axes ^{a} can be transformed to the orthogonal body frame ^{b} by 6 small angles (after [14]).

Defining the body frame so that the x-axis coincides and y^b-axis lies in the plane spanned by x^a and y^a (3) reduces to:

$$f^b = \boldsymbol{T}_a^b f^a \,, \quad \text{with} \quad \boldsymbol{T}_a^b = \begin{bmatrix} 1 & -\alpha_{yz} & \alpha_{zy} \\ 0 & 1 & -\alpha_{zx} \\ 0 & 0 & 1 \end{bmatrix} . \tag{4}$$

This gives a 9-parameter model by extending (1) with (4):

$$f^s = \boldsymbol{S}_f \boldsymbol{T}_a^{b\,-1} f^b + \boldsymbol{b}_f + \boldsymbol{v}_f \,, \tag{5}$$

3. Leveling

Following equations are used for accelerometer levelling [3], which describe the orientation of the IMU body frame with respect to the local tangent navigation frame denoted by ^{n}. Euler angles are used to describe the attitude using *roll* ϕ_{nb}, *pitch* θ_{nb} and *yaw* ψ_{nb} rotations.

$$\begin{aligned} \phi_{nb} &= \operatorname{atan}_2\left(-f_y^b, -f_z^b\right) \\ \theta_{nb} &= \operatorname{atan}\left(\frac{f_x^b}{\sqrt{f_y^{b\,2} + f_z^{b\,2}}}\right) \end{aligned} \tag{6}$$

Note that `arctan2()` must be used for roll computation, but if limiting tilting to the upper half sphere it can be replaced by `arctan()`.

For this case study we suppose the yaw is exactly known, so $\psi_{nb} = 0$ is used with zero variance throughout the rest of this paper.

The partial derivatives of this model are:

$$\boldsymbol{F}_{\phi\theta} := \begin{bmatrix} \frac{\partial \phi}{\partial f^b} \\ \frac{\partial \theta}{\partial f^b} \end{bmatrix} = \begin{bmatrix} 0 & \frac{f_z^b}{f_y^{b\,2} + f_z^{b\,2}} & \frac{-f_y^b}{f_y^{b\,2} + f_z^{b\,2}} \\ \frac{f_{yz}}{f_{xyz}^2} & \frac{-f_x^b f_y^b}{f_{xyz}^2 f_{yz}} & \frac{-f_x^b f_z^b}{f_{xyz}^2 f_{yz}} \end{bmatrix} , \quad \text{with} \quad \begin{aligned} f_{yz} &= \sqrt{f_y^{b\,2} + f_z^{b\,2}} \\ f_{xyz}^2 &= f_x^{b\,2} + f_y^{b\,2} + f_z^{b\,2} \end{aligned} . \tag{7}$$

3.1. Variance Propagation

In Figure 2 we investigate angle accuracy of roll and pitch with respect to roll and pitch if accelerometer noise is assumed to be equal for all three axis and .

This seems a legit assumption for consumer-grade MEMS IMUs, especially $\sigma_{f^b}^2 = 0.002^2 \left[m^2/s^4\right]$ predominant static applications where lower measurement rates can be used.

One can see that an accuracy of 13 mgon can be achieved in the vicinity of the zenith direction. Interestingly tilting to the side (producing roll) does not effect both accuracies. On the other hand pitching the pole deacreases roll accuracy quadratically.

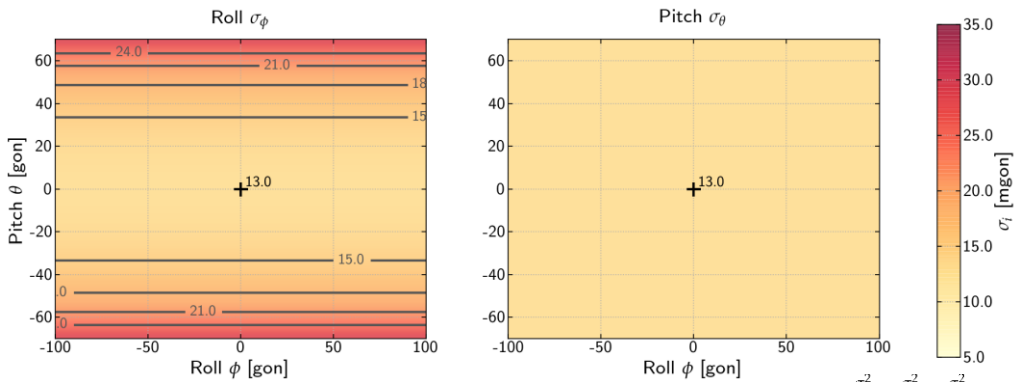

Fig. 2 Accuracy of Roll ϕ_{nb} **(left)** and Pitch θ_{nb} **(right)** with uniform accelerometer noise $\sigma_{f_x^b}^2 = \sigma_{f_y^b}^2 = \sigma_{f_z^b}^2$ of $0.002^2 \left[m^2/s^4\right]$.

Figure 3 shows the linear increase of the tilt angle standard deviation with increasing accelerometer noise for a tilted attitude of $\phi_{nb} = 0\,[\text{gon}]$, $\theta_{nb} = 50\,[\text{gon}]$.

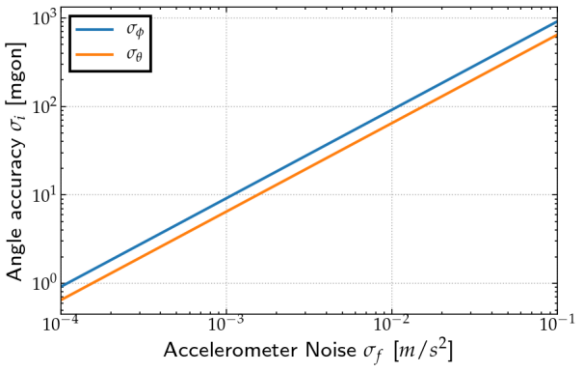

Fig. 3 Tilt angle accuracies with respect to accelerometer noise for $\phi_{nb} = 0\,[\text{gon}]$, $\theta_{nb} = 50\,[\text{gon}]$.

3.2. Sensitivity Analysis

Sensitivity analysis can be used to analyze the relations between input and output parameters of a model [27], in our case $[\phi, \theta] = \varphi(\boldsymbol{f}^b)$. Goals of sensitivity analysis are listed in [27]:

- Model validation,
- Model optimization, and
- Identification of important parameters

These has been ported to the engineering geodesy context by [28] and has been used in many studies since then (e.g. [28, 29, 30]). Please refer to these references for details of the methodology and implementation details. The sensitivity measure S_i^j for the *i*-th input measure X_i on the *j*-th output Y_j can be computed using

$$S_i^j = 1 - \frac{\sigma^2_{E(Y_j|X_{\neg i})}}{\sigma^2_{Y_j}}\,. \tag{8}$$

Here $\sigma^2_{Y_j}$ describes the variance of the output parameter and $\sigma^2_{E(Y_j|X_{\neg i})}$ describes the variance of the conditional expectation value, where all input parameters except X_i are fixed.

Considering a parameter free model of $f^s = f^b + v_f$ one can plot the sensitivities/influences of each of the accelerometer measurements on the two output angles ϕ_{nb} and θ_{nb} (s. Figure 4).

The subplots of Figure 4 correspond approximately to the elements of (7). What we can derive from this can be summarized as follows:

- Accelerometer x-axis does not influence ϕ_{nb} computation (compare (6)).
- But is prominent for θ_{nb} for small pitches no matter which ϕ_{nb}.
- Influences of accelerometer measurements on roll computation are independent from pitch.
- For ϕ_{nb} computation f_y is important up to 50 [gon] at which point f_y and f_z are equally important. For higher rolls f_z gains importance.
- For smaller tilt angles < 30 [gon] z-accelerometer reading is inessential for both tilt angles, whilst y-accelerometer is dominant for roll ϕ_{nb} and x-accelerometer is dominant for pitch θ_{nb} computation.

The above conclusions can be verified geometrically and especially the last one can be accounted for in designing calibration schemes.

To get an idea of the importance of the different sensor model parameters when it comes to accelerometer-leveling we have setup a simulation framework, where we can simulate accelerometer measurements according to the models of Section 2. This enables us to perform sensitivity analysis on the 9-parameter model from (5) and the leveling equations (6). The stochastic model has been chosen in accordance to the calibration simulation results from Section 4. Also the simulated quantities are given in Section 4.

Results from the Variance based sensitivity analysis for the

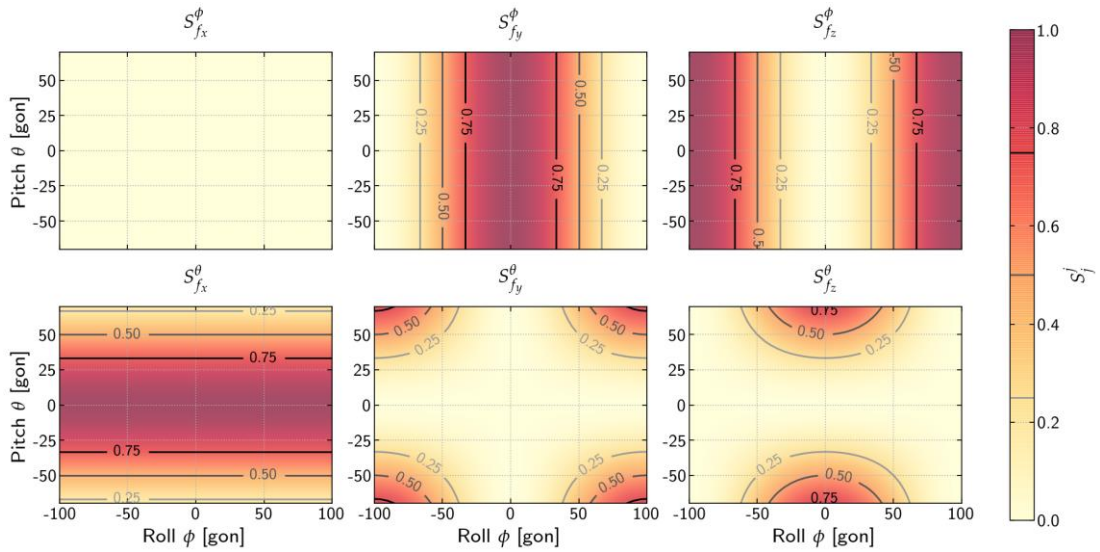

Fig. 4 Total effects of accelerometer measurements $\mathbf{f}^b$ for output quantities roll ϕ_{nb} **(upper)** and pitch θ_{nb} **(lower)** with respect to tilt.

9-parameter model (5) are shown in Figure 5 for Roll and in Figure 6 for Pitch at a log scale. Because of the fact that sensitivity quantities are symmetric in both roll- and pitch-axis, only subplots for positive pitches are shown.

As before in Figure 4 we can deduce that the measured forces f_y and f_z in blue are important for roll computation. Moreover the first misalignment parameter α_{zx} in red has a big share on the total variance of ϕ_{nb}. The bias and scale error terms of y and z have an influence of at least one magnitude lower (about 1 to 8%) than the three first listed quantities. The bias shows a quite similar behavior over different ϕ_{nb} and θ_{nb} to the measured forces.

attitudes.

To sum up, scale parameters might be of lowest importance when it comes to accelerometer leveling and special care of misalignment parameters must be taken.

4. Calibration

For the following investigations, the multi-position scheme from [24] is used, where they propose a 24-position calibration scheme. This scheme distributes the measured

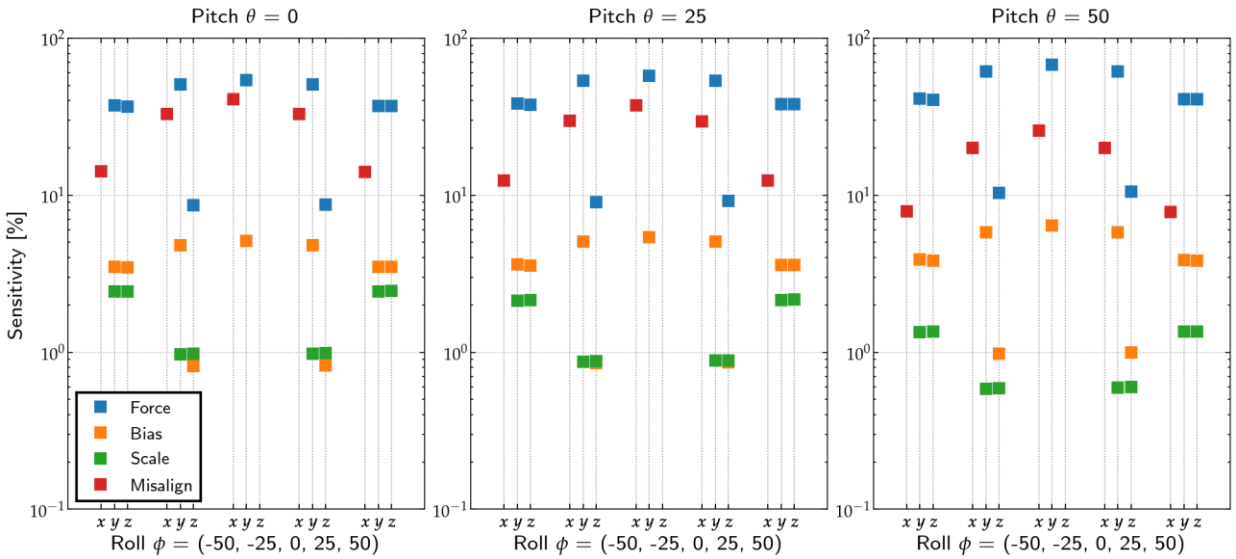

Fig. 5 Effects of all sensor model parameters on Roll ϕ_{nb} .

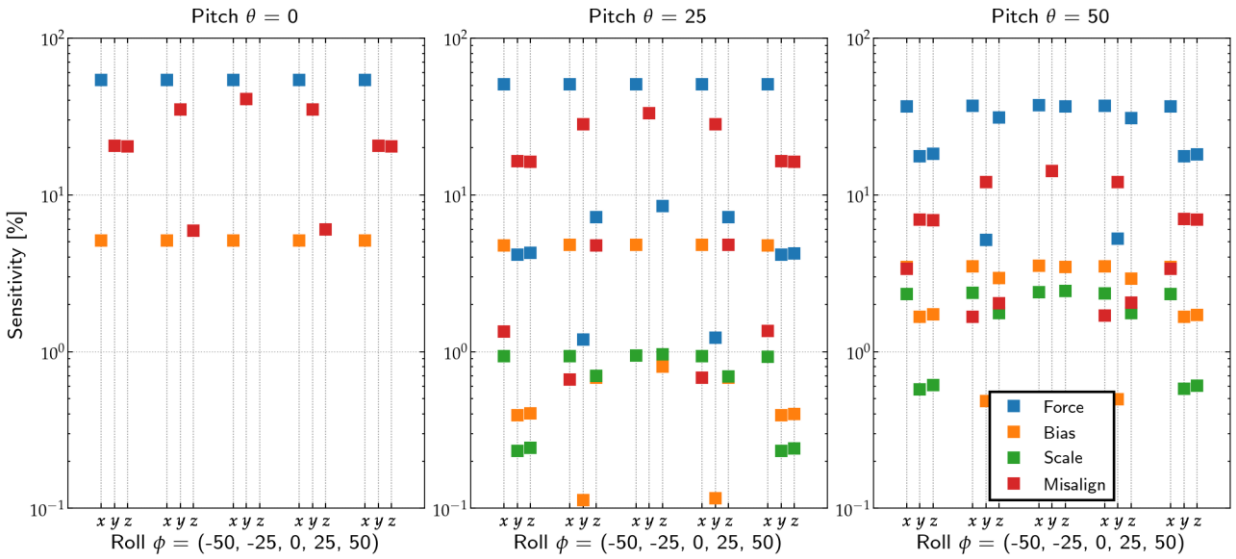

Fig. 6 Effects of all sensor model parameters on Pitch θ_{nb} .

Concerning pitch computation we can see a similar order of importance. After measured forces (and especially f_x) again misalignment parameters (α_{zy} and α_{zx}) are of relevance. Scale parameters stay below 3% for all investigated

g-vector evenly in the unit-sphere. Subsequent simulations are done using the stochastic model from Section 3.1, simulating 2 seconds of data acquisition per attitude and error

parameters of $\tilde{\boldsymbol{\alpha}}_f = [12 \quad 12 \quad 44]\ [mgon]$, $\tilde{\boldsymbol{b}}_f = [0.05 \quad 0.01 \quad 0.03]\ [m/s^2]$, and $\tilde{\boldsymbol{s}}_f = [200 \quad 200 \quad 200]\ [ppm]$.

4.1. Gravity based

The **gravity-based** approach uses the fact, that the measured gravity must be independent from attitude of the IMU.

$$\varphi(\boldsymbol{l}, \boldsymbol{x}) = \sqrt{f_x^{b2} + f_y^{b2} + f_z^{b2}} - g = 0 \tag{9}$$

The disadvantage of these approaches as, that g must be known. Generally, no exact measurement of g is available, but values from theoretical models can be computed. Model (9) can be used in a Gauss-Helmert-Adjustment (GH) to estimate the different model parameters of the tri-axial accelerometers of (5).

4.2. Robot aided

Using an industrial robot as additional equipment adds two more observations from robot encoders ϕ_r and θ_r with a standard deviation of 3.2 [mgon].

$$\boldsymbol{\varphi}(\boldsymbol{l}, \boldsymbol{x}) = \begin{bmatrix} \operatorname{atan}_2\left(f_y^b, -f_z^b\right) - \phi_r \\ \operatorname{atan}\left(\frac{f_x^b}{\sqrt{f_y^{b2}+f_z^{b2}}}\right) - \theta_r \\ \sqrt{f_x^{b2} + f_y^{b2} + f_z^{b2}} - g \end{bmatrix} = \mathbf{0} \tag{10}$$

The degree of freedom does not change, since two observations and two equations are added to the model per position/attitude.

Comparing these two approaches using simulation, we can see the biggest advantage on determination of misalignment parameters (see Figure 7). Expected bias accuracy is reduced by about 50%, Scale accuracy by about 30% and Misalignment by about 70%. Considering the value of scale parameters of 200 [ppm] and the standard deviation a-posteriori we can deduce that scale parameters are poorly determinable. Additional equipment only with reference attitude measurements can not improve this situation. The biases can be very well estimated, since σ_b is about two orders of magnitude smaller than the simulated true values. For the misalignment parameters we can see very high estimation errors (and corresponding standard deviations) for the gravity based approach. This is were the biggest benefit of additional reference tilting measurements can be seen.

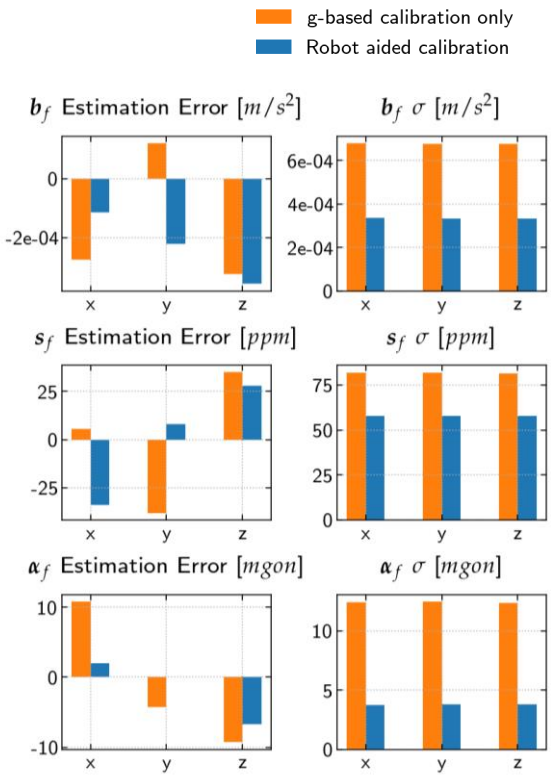

Fig. 7 Comparison of the two IMU calibration approaches. On the **(left)** printed are the estimation errors from one simulation. On the **(right)** are the standard deviations of parameters from GH-adjustment.

The correlation structure of the estimated error parameters for both approaches is shown in Figure 8. The estimated parameters of the gravity-based approach are already nearly uncorrelated. This is due to the evenly designed multi-position scheme. Only the scale parameters are correlated by about 0.2. This correlation can be reduced by one order of magnitude using the robot-aided calibration.

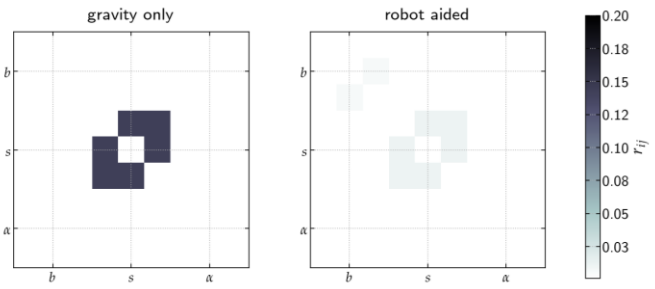

Fig. 8 Correlation Coefficient matrices $\operatorname{abs}(\operatorname{corr}(\boldsymbol{\Sigma}_{xx})) - \boldsymbol{I}$ of the parameters for gravity based **(left)** and robot aided **(right)** calibration simulation.

5. Conclusion and Outlook

A simulation framework has been set up to simulate tri-axial accelerometer data according to the different sensor models found in literature. Using this simulation framework, we have first analyzed how well the two tilting angles roll ϕ_{nb} and pitch θ_{nb} can be determined. For small tilting angles (in the vicinity of zenith direction) an accuracy of 13 mgon can be

achieved if accelerometer with uncertainty of 0.002 m/s (standard deviation) are available, which might be feasible with averaging over static timespan. We found out that pitch accuracy is independent of current roll and pitch and that roll accuracy decreases with growing roll.

Using a 9-parameter sensor model for an accelerometer triad the sensitivity of the tilting angles with respect to these sensor model parameters has been investigated using variance based sensitivity analysis. This method revealed that for smaller tilt angles < 30 [gon] only the measured forces of f_y for roll and f_x for pitch are important. Concerning the 9-parameter sensor model the first misalignment parameter α_{zx} show the biggest influence on roll computation. Based on the calibrations simulation results bias and scale parameters are not that important. A comparable conclusion can be drawn for pitch computation, so in general special care must be taken of the three misalignment parameters of the accelerometer triad sensor model.

As a consequence we have analyzed two accelerometer calibration approaches using the same simulation framework. A gravity-only based calibration approach (which can be applied in-field) has been compared with a calibration process aided by an industrial robot. These two calibration procedures are implemented as a GH-adjustment and the studies shows, that especially for those misalignment parameters an aided calibration in laboratory brings an improvement of about 70%.

Future steps would be to test calibration procedures with real hardware. Furthermore, an evaluation experiment for tilt estimation using MEMS IMU should be designed. An idea could be to use the acquired knowledge from sensitivity analysis to optimize the calibration process in terms of economics and time saving. In combination with a recursive least squares approach one might relax the position scheme and adjust it to the given needs. Findings from variance propagation and sensitivity analysis might be used in further studies on pole tilt estimation and compensation both for total stations and GNSS.

References

[1] Jekeli, C. (2012). Inertial navigation systems with geodetic applications. Walter de Gruyter.

[2] Hofmann-Wellenhof, B., Legat, K., & Wieser, M. (2011). Navigation: principles of positioning and guidance. Springer Science & Business Media.

[3] Jekeli, C. (2012). Inertial navigation systems with geodetic applications. Walter de Gruyter.

[4] Alam, F., Zhaihe, Z., & Jiajia, H. (2014). A Comparative Analysis of Orientation Estimation Filters using MEMS based IMU. 2nd International Conference on Research in Science, Engineering and Technology (ICRSET'2014), 86–91.

[5] Wilczyńska, I., & Ćmielewski, K. (2016). Modern measurements techniques in structural monitoring on example of ceiling beams. In Proceedings of the 3rd Joint International Symposium on Deformation Monitoring (JISDM), Vienna, Austria (Vol. 30).

[6] Sekiya, H., Kinomoto, T., & Miki, C. (2016). Determination method of bridge rotation angle response using MEMS IMU. Sensors (Switzerland), 16(11), 1–13. https://doi.org/10.3390/s16111882

[7] Engel, P., Foppe, K., & Köster, U. (2018). Multisensorsystem zur Erfassung von Turmschwingungen an der Marienkirche Neubrandenburg. In MST 2018 - Multisensortechnologie: Low-Cost Sensoren im Verbund, DVW-Schriftenreihe, Band 92 (pp. 167–168). Augsburg.

[8] Kargoll, B., Omidalizarandi, M., Loth, I., Paffenholz, J.-A., & Alkhatib, H. (2018). An iteratively reweighted least-squares approach to adaptive robust adjustment of parameters in linear regression models with autoregressive and t-distributed deviations. Journal of Geodesy, 92(3), 271–297.

[9] Luo, X., Schaufler, S., Carrera, M., & Celebi, I. (2018). High-Precision RTK Positioning with Calibration-Free Tilt Compensation High-Precision RTK Positioning with Calibration-Free tilt Compensation. In FIG Congress 2018 - Embracing our smart world where the continents connect.

[10] Viney, I. T., & Jackson, P. R. (1999). Method and apparatus for precision location of GPS survey tilt pole. Google Patents.

[11] Groves, P. D. (2013). Principles of GNSS, inertial, and multisensor integrated navigation systems. Artech house.

[12] Gleason, S., & Gebre-Egziabher, D. (2009). GNSS applications and methods. Artech House.

[13] Wendel, J. (2011). Integrierte Navigationssysteme. Oldenbourg Verlag München.

[14] Skog, I., & Händel, P. (2006). Calibration of a MEMS inertial measurement unit. Signal Processing, 17–22.

[15] Syed, Z. F., Aggarwal, P., Goodall, C., Niu, X., & El-Sheimy, N. (2007). A new multi-position calibration method for MEMS inertial navigation systems. Measurement Science and Technology, 18(7), 1897–1907. https://doi.org/10.1088/0957-0233/18/7/016

[16] Torayashiki, O., & Komaki, K. (2007). Inertial Sensors. Reliability of MEMS, (December), 205–223. https://doi.org/10.1002/9783527622139.ch7

[17] Zhang, H., Wu, Y., Wu, W., Wu, M., & Hu, X. (2010). Improved multi-position calibration for inertial measurement units. Measurement Science and Technology, 21(1), 015107. https://doi.org/10.1088/0957-0233/21/1/015107

[18] Kim, A., & Golnaraghi, M. F. (2004). Initial calibration of an inertial measurement unit using an optical position tracking system. Position Location and Navigation Symposium, 2004. PLANS 2004, 96–101.

[19] Lv, J., Ravankar, A. A., Kobayashi, Y., & Emaru, T. (2017). A method of low-cost IMU calibration and alignment. SII 2016 - 2016 IEEE/SICE International Symposium on System Integration, 373–378.

[20] Fong, W. T., Ong, S. K., & Nee, a Y. C. (2008). Methods for in-field user calibration of an inertial

measurement unit without external equipment. Measurement Science and Technology, 19(8), 085202. https://doi.org/10.1088/0957-0233/19/8/085202

[21] Lötters, J. C., Schipper, J., Veltink, P. H., Olthuis, W., & Bergveld, P. (1998). Procedure for in-use calibration of triaxial accelerometers in medical applications. Sensors and Actuators, A: Physical, 68(1–3 pt 2), 221–228.

[22] Shin, E. H., & El-Sheimy, N. (2002). A new calibration method for strapdown inertial navigation systems. Zeitschrift Für Vermessungswesen, 127(1), 41–50.

[23] Qureshi, U., & Golnaraghi, F. (2017). An Algorithm for the In-Field Calibration of a MEMS IMU. IEEE Sensors Journal.

[24] Cai, Q., Song, N., Yang, G., & Liu, Y. (2013). Accelerometer calibration with nonlinear scale factor based on multi-position observation. Measurement Science and Technology, 24(10). https://doi.org/10.1088/0957-0233/24/10/105002

[25] Pretto, A., & Grisetti, G. (2014). Calibration and performance evaluation of low-cost IMUs. 18th International Workshop on ADC Modelling and Testing.

[26] Tedaldi, D., Pretto, A., & Menegatti, E. (2014). A robust and easy to implement method for IMU calibration without external equipments. In Robotics and Automation (ICRA), 2014 IEEE International Conference on (pp. 3042–3049).

[27] Saltelli, A., Tarantola, S., Campolongo, F., & Ratto, M. (2004). Sensitivity Analysis In Practice. John Wiley & Sons.

[28] Schwieger, V. (2007). Sensitivity analysis as a general tool for model optimisation – examples for trajectory estimation. Journal of Applied Geodesy, 1(1), 27–34. https://doi.org/10.1515/jag.2007.004

[29] Ramm, K. (2008). Evaluation von Filter-Ansätzen für die Positionsschätzung von Fahrzeugen mit den Werkzeugen der Sensitivitätsanalyse. Universität Stuttgart.

[30] Beetz, A. (2012). Ein modulares Simulationskonzept zur Evaluierung von Positionssensoren sowie Filter- und Regelalgorithmen am Beispiel des automatisierten Straßenbaus. Universität Stuttgart.